Separation and Purification Technology 330 (2024) 125261

Contents lists available at ScienceDirect

Separation and Purification Technology

journal homepage: www.elsevier.com/locate/seppur

Analysis of CO_2 hydrate formation from flue gas mixtures in a bubble column reactor

Awan Bhati, Aritra Kar, Vaibhav Bahadur *

Walker Department of Mechanical Engineering, The University of Texas at Austin, USA

ARTICLE INFO

Editor: S. Yi

Keywords:
CO_2 hydrate formation
Bubble column reactor
Flue gas
Conversion factor
Carbon capture and sequestration

ABSTRACT

Gigascale carbon capture and sequestration (CCS) is increasingly seen as essential to meeting the targets of the Paris Agreement. As an alternative to conventional CCS approaches, carbon dioxide (CO_2) hydrates have received attention as materials which can enable new approaches to carbon capture as well as carbon sequestration. CO_2 hydrates (ice-like materials of CO_2 and water) form at medium pressures (<400 psi) and temperatures of >0 °C from a water-CO_2 mixture. Bubble column reactors (BCR) have been studied as a preferred way of forming CO_2 hydrates. This study uses an inhouse, recently-developed modeling framework to predict performance of a BCR for CO_2 hydrate formation from flue gas (CO_2/N_2), and pure CO_2 streams. We highlight and analyze specific aspects of hydrate formation that are important for CO_2 sequestration, and for CO_2 separation/capture. In particular, two performance parameters are analyzed: i) gas consumption rate for hydrate formation (normalized with reactor volume), and ii) fraction of CO_2 that converts to CO_2 hydrates in a single pass (conversion factor). The first metric quantifies the overall productivity of a BCR by obtaining the net CO_2 that can be sequestered or separated from the flue gas stream. The second metric relates to the efficiency of the system by quantifying the need for recirculation and the quality of the exit stream after a single pass. Extensive parametric analysis is conducted to study the influence of pressure, temperature, CO_2 mole fraction at inlet, gas flow rate and reactor geometry on hydrate formation. Across the range of simulations conducted in this study, the highest gas consumption rate per unit reactor volume was 28.9 ton/yr/m^3 and the highest conversion factor was 67.8 %. Both parameters increase with increasing pressure, decreasing temperature and increasing inlet mole fraction of CO_2. Increasing gas flow rate increases the gas consumption rate (i.e., hydrate formation rate) but reduces the conversion factor. This suggests that the overall productivity of BCRs increases with gas flow rate at the expense of its efficiency. Reduced efficiency increases recirculation-related costs and high flow rate increases compression and cooling costs. For flue gas, increasing the reactor volume by increasing the height or diameter increases conversion factor but significantly reduces the gas consumption rate per unit reactor volume. For pure CO_2, increasing the reactor height increases the conversion factor without changing the volumetric gas consumption rate. Decreasing the diameter increases volumetric gas consumption rate without changing the conversion factor. These findings suggest that compact reactors are more suitable for CO_2 hydrate slurry production (on a volumetric basis), while larger reactors are suitable for CO_2 separation/capture applications. Overall, this study provides a basis for the design and operation of BCRs for CO_2 hydrates-based CCS applications.

1. Introduction

Gigascale carbon capture and sequestration (CCS) is increasingly being considered as critical to meeting the goals of the Paris Agreement [1,2]. Current operational CCS capacity is ~40 Mton/yr, which is negligible compared to the projected need for upto10 Gton/yr capacity by 2050 [2]. This highlights the need for rapid deployment of CCS technologies which are at a commercial stage. However, existing technologies have significant limitations associated with them, highlighting the need for novel approaches throughout the entire CCS ecosystem. This study focuses on CCS from flue gas streams, noting that over 60 % of CO_2 emissions are generated by power plants [3], where the exhaust is predominantly a mixture of N_2 and CO_2 (alongside H_2O and O_2). While the CO_2 concentration in flue gas ranges from 10 to 20 %, certain exhaust gases produced have CO_2 concentrations of up to 95 % [4,5]. Flue gas from the oxy-fuel combustion of a fuel in a mixture of oxygen and recycled flue gas can contain CO_2 concentrations as high as

* Corresponding author.
E-mail address: vb@austin.utexas.edu (V. Bahadur).

https://doi.org/10.1016/j.seppur.2023.125261
Received 5 July 2023; Received in revised form 11 September 2023; Accepted 29 September 2023
Available online 1 October 2023
1383-5866/© 2023 Elsevier B.V. All rights reserved.

Nomenclature

A_b	Surface area of bubble
A_{cs}	Reactor cross sectional area
A_f	Hydrate film area
c	Gas concentration of CO_2
c_{eq}	Equilibrium gas concentration of CO_2
C_D	Drag coefficient
D	Reactor diameter
g	Acceleration due to gravity
g_f	Growth factor (=0.25)
ΔH	Heat of hydrate formation
H	Height of water column in reactor
h_{side}	Heat transfer coefficient on the side
h_{top}	Heat transfer coefficient on the top
k	Thermal conductivity of water
k_m	Mass transfer coefficient
M	Mass of hydrate on the bubble
M_h	Molar mass of hydrate
M_{CO_2}	Molar mass of CO_2
$\dot{m}_{gcr}$	Gas consumption rate of the reactor
n_{N_2}	Moles of non-participating gas (N_2)
N	Number density of bubbles
P	Total pressure inside the bubble
P_{eq}	Equilibrium pressure
P_{op}	Operating pressure of the reactor
Q	Gas flow rate per unit area or gas flux
$\dot{Q}$	Gas flow rate
r	Radial coordinate
R	Radius of the reactor
$\overline{R}$	Universal Gas Constant
t	Film thickness
T	Temperature
T_{inf}	Temperature of coolant
T_{top}	Temperature at top in the headspace of reactor
T_{pc}	Temperature of inlet gas
T_{amb}	Operating temperature
v	Velocity of the bubble
v_{term}	Terminal velocity
V_R	Total volume of the reactor
x	Mole fraction of CO_2
x_i	Mole fraction of CO_2 at inlet
z	Axial coordinate
Z	Compressibility factor
$Z_{eq} = Z(P_{eq},T)$	Compressibility factor at equilibrium
γ	Gas water surface tension
η	Bubble radius
η_{CF}	Percentage conversion factor
η_s	Bubble radius at sparger exit
ρ_w	Density of water
ρ_g	Density of gas

70 % [6]. Flue gas from refineries, cement, and steel production plant have CO_2 concentrations ranging from 10 to 35 % [7,8]. It is noted that the major components of flue gas are always CO_2 and N_2; CO_2 needs to be separated (captured) from this stream before being sequestered.

This manuscript focuses on the use of CO_2 hydrates for CCS from flue gas (represented by CO_2/N_2 mixtures). Clathrate hydrates are water-based crystalline solids consisting of a guest molecule (e.g., methane, CO_2, ethane, tetrahydrofuran, cyclopentane, etc.) trapped in a lattice of water molecules [9-11]. Depending upon the lattice structure, upto 6 water molecules can be needed to trap 1 molecule of CO_2. CO_2 hydrates visually resemble ice and form at medium pressures (400 psi) and low temperatures (0–4 °C) in a water and CO_2 environment [10]. Hydrates can enable several applications in the areas of CCS, water desalination, gas separation, storage and transportation [12]. This manuscript studies CO_2 hydrates from both carbon sequestration as well as CO_2 separation/capture standpoints [13-15].

The current state-of-the-art for CO_2 sequestration is CO_2 injection as supercritical CO_2 in depleted oil reservoirs [16,17]. Although a well-established technology, it has multiple limitations and challenges which include high pressure requirements, high monitoring cost to prevent leakage, lack of available storage sites, requirements for high purity CO_2, etc. [16,17]. Other sequestration options being developed include CO_2 mineralization, biologic approaches and embedding CO_2 in materials. While all these approaches are very promising, they all have their disadvantages. There is enormous scope for the development of novel sequestration approaches to add to the existing basket of solutions, particularly in view of the gigascale capacity requirements.

The solid, immobile nature and relatively lower pressure requirement of CO_2 hydrates makes it a viable option for CO_2 storage. 1 kg of solid CO_2 hydrate can sequester upto 290 g of CO_2 (i.e. 150 L of CO_2 at 25 °C & 1 atm) [18]. Potential pathways for CO_2 storage as hydrates have been discussed in detail in recent literature [14,19]. Sequestration sites for CO_2 hydrates include seabed locations with appropriate P-T conditions, sub-seabed storage, permafrost regions, and depleted gas fields [14]. Another option involves injecting CO_2 into CH_4 hydrate reservoirs to achieve CO_2 hydrate formation and methane production simultaneously [20,21]. CO_2 storage efficiency as high as 96.7 % (irrespective of initial methane hydrate saturation) was reported using this approach [22]. Laboratory tests for CO_2 hydrate formation have shown that hydrates form more easily from CO_2 gas as opposed to liquid CO_2 [23]. Field tests with CO_2 hydrates have also been conducted [16]. It was found that this concept is suitable when the produced hydrate does not have trapped gas, in which case it is denser than seawater [16,24]. Hydrate formed from water saturated with CO_2 is also much more denser than otherwise [25]. Field experiments have been conducted at ocean depths of 1000–1300 m in Monterey Bay, CA, using liquid CO_2, water, and solid CO_2 hydrate [26]. Importantly, to make this concept economically viable, rapid formation of compact CO_2 hydrates is needed.

Hydrates have also been explored for applications in the separation or capture of CO_2 from gas mixtures [14,27,28]. Hydrates-based CO_2 capture has been studied for separation from syngas (CO_2/H_2 mixture) [29,30], biogas [31 32], natural gas (CO_2/CH_4 mixture) [33,34], and flue gas (CO_2/N_2 mixture) [35-37]. Separation of as much as 80 % of the inlet CO_2 in syngas was reported using Tetrabutylammonium bromide (TBAB) as a chemical promoter [38]. This is possible since the formation of CO_2 hydrates is easier (thermodynamically) than hydrates of H_2, N_2, CH_4, C_2H_6, etc. The dissociation heat and equilibrium curve for hydrate formation with CO_2/N_2 mixtures in the presence and absence of chemical promoters like tetrahydrofuran (THF) and TBAB have been reported [5,27,39,40]. Even for CO_2-lean mixtures (as lean as 87 % N_2, 13 % CO_2), the hydrate formed is expected to have a molecular formula of $5.43CO_2.1.89\ N_2{\cdot}46H_2O$ [39,41]; this shows high selectivity of CO_2 absorption from CO_2/N_2 binary hydrates. It was found that CO_2 selectivity reduces upon adding chemical promoters like THF and TBAB. While promoters reduce the required pressure and induction time for CO_2 hydrate [30,37], they also reduce CO_2 selectivity, reduce growth rate [37] and can pose environmental challenges.

Rapid hydrate formation is critical for all hydrates-based CCS applications [17]. There are various ways to promote hydrate formation, apart from using chemical promoters. These include bubbling CO_2, stirring, spraying water in a CO_2-filled column, and distributing water in

porous materials [42-44]. As an illustration, the use of silica gel with different pore sizes has been studied for CO_2 capture from flue gas [15]. It was found that larger pore sizes helped increase the total gas consumption and separation. A silica sand bend with water was found to have a significantly higher formation rate than a stirred vessel [45]. Hydrate formation using a water spraying apparatus has been studied with different nozzle atomizing angles, water volumes, etc.; it was found that larger atomization angle favors faster hydrate formation [46]. CO_2 separation from flue gas using hydrate formation in fine sediments has been studied [47]. It was seen that while N_2 can also form hydrates alongwith CO_2, it is feasible to capture CO_2 from CO_2/N_2 mixtures using hydrate formation. A mechanically agitated gas-inducing crystallizer was developed [48] that combined the benefits of stirring and bubbling; however the power required for mechanical agitation significantly hurt the viability of this concept.

Bubble column reactors (BCR) involve bubbling gases into liquids, which requires much less energy than mechanical agitation [29]. There exist limited experimental studies of BCR-based CO_2 separation, via hydrate formation from syngas (CO_2 + H_2) [29,30]. In general, most studies on CO_2 separation from flue gas use mechanical stirring and do not involve BCRs [49,50]. The influence of Fe_3O_4 nanoparticles on CO_2 absorption from flue gas in a BCR has been experimentally studied [51]. An examination of modeling-based studies again shows limited numerical studies [52,53] on BCRs, especially those related to CO_2 capture from flue gas. Overall, there is a clearly a lack of experimental and modeling studies on BCR-based CCS from flue gas.

This modeling study aims at a detailed understanding of various aspects of BCR-based CCS from flue gas. An inhouse, validated numerical modeling framework [52,53] developed by the present group is used to analyze BCR-based hydrate formation for CCS from flue gas. In particular, two performance metrics of BCRs are quantified and analyzed. The first is the gas consumption rate of CO_2 (to form CO_2 hydrates) per unit reactor volume ($\dot{m}_{gcr}$). This parameter evaluates the overall productivity of the BCR and determines the rate at which CO_2 can be captured or sequestered. The second metric is the conversion factor (η_{CF}), i.e., the fraction of inlet CO_2 converted to hydrates in a single pass. This is linked to the efficiency of the process. While increasing the overall productivity is important, a reduced efficiency increases costs related to recirculation, compression, water requirement, etc. While both these metrics are important for both carbon separation and carbon sequestration applications, a carbon sequestration application would focus more on enhancing $\dot{m}_{gcr}$, as the primary objective is to rapidly produce hydrates for sequestration.

On the other hand, a carbon separation application would emphasize η_{CF}, as that governs the need for further separation and recirculation. Understanding various tradeoffs associated with these two related metrics is critical. This study considers a wide range of operating conditions, geometry, and inlet CO_2 concentrations to assess performance with respect to both of these performance metrics. This study concludes with simulation results on hydrate formation from pure CO_2, which would be the focus of a sequestration application. We note that the use of seawater for hydrate formation is highly desirable. However, the presence of salt slows hydrate formation kinetics [54], besides there is no experimental study on saltwater-based hydrate formation from flue gas in a BCR. Therefore, this study simulates the use of pure water for hydrate formation. We note that even though hydrate formation will slow down with saltwater, the key trends reported in this work will still be valid.

It is noted that none of the previous BCR-based studies (for syngas), analyzed performance as a function of inlet CO_2 concentration. This is a key parameter in the CCS process stream, especially for a hydrates-based CCS system where the same reactor can be used for both CO_2 capture and CO_2 sequestration applications. In a conventional CCS plant, the carbon capture site has to refine CO_2 from flue gas to high purity, which is then sent for sequestration. Existing sequestration approaches (injection, mineralization) require high purity (>95 % CO_2). The cost of refining CO_2 to >95 % from lower concentrations (~20–50 %) is a significant contributor to the overall cost of a CCS project [17]. Also, separation/capture techniques do not always yield high purity CO_2. A hydrates-based CCS system which can simultaneously purify and sequester CO_2 can reduce the overall cost of CCS by reducing purification costs. The findings and insights from this study can facilitate the design and optimization of BCRs to enable such novel approaches for CCS of flue gas streams.

2. Mathematical model of hydrate formation

Fig. 1a shows a schematic of a BCR, where bubbles of flue gas are sparged from the bottom. BCRs involve continuous hydrate formation where the hydrate slurry can be collected from either the gas–liquid interface or from the bottom of the reactor (as hydrates settle down). The mathematical model for hydrate formation in a BCR has been extensively described in a previous study [52,53] from this group; a high-level summary of the model is provided ahead. Hydrate formation from a CO_2/N_2 mixture is modeled with the assumption that CO_2 selectively forms hydrates while N_2 remains non-participatory. The model uses the equilibrium curve for CO_2-pure water-hydrate. Other assumptions involved in the model are described in [52,53]. Fig. 1b shows the computational domain where the mathematical model (described below) is solved under steady-state conditions.

2.1. Governing equations

The governing equations for the system consist of 6 equations and 6 variables, i.e., v, η, m, x, N, T. Equation (1) describes the velocity field of the bubble and is based on a force balance involving gravity, buoyancy, acceleration and drag on the bubble. The bubble is assumed to have terminal velocity as it escapes the sparger.

$$\left(m+\frac{4}{3}\pi\rho_g\eta^3\right)v\frac{\partial v}{\partial z}=\left(\rho_w-\rho_g\right)\frac{4}{3}\pi\eta^3 g-mg-\frac{1}{2}\rho_w C_D A_b v^2 \qquad BC: v(0)=v_{term} \tag{1}$$

The bubble radius evolution in the reactor is tracked using compressible gas law while accounting for hydrate crystallization using equation (2). The Peng-Robinson equation of state is used to evaluate the compressibility factor (Z) as described in [55,56]. The bubble diameter, as it escapes the sparger at $z=0$ is assumed to be fixed at $\eta_s=150$ μm for all flue gas mixtures considered in this study.

$$\left(3P-\frac{2\gamma}{\eta}\right)\frac{\partial\eta}{\partial z}=-\frac{3Z\overline{R}T}{4\pi\eta^2M_h}\frac{\partial m}{\partial z}+\rho_w g_\eta+\frac{P\eta}{T}\frac{\partial T}{\partial z} \qquad BC: \eta(0)=\eta_s \tag{2}$$

Equation (3) uses concentration driving force to evaluate the hydrate mass attached to the bubble. Hydrate crystallization is evaluated using film growth model on the surface of the bubble and the hydrate mass is assumed to be collected and concentrated at the bottom of the bubble [57]. The bubble is assumed to have no hydrate as it leaves the sparger at $z=0$; nucleation is assumed to occur at the instant that it enters the BCR.

$$v\frac{\partial m}{\partial z}=k_m M_h A_f\left(xc-c_{eq}\right), A_f=2\pi\eta g_f t, c=\frac{P}{Z\overline{R}T}, c_{eq}=\frac{P_{eq}}{Z_{eq}\overline{R}T} \qquad BC: m(0)=0 \tag{3}$$

Equation (4) is used to evaluate the mole fraction (x) of CO_2 by assuming N_2 as a non-participating gas and x_i as the mole fraction of CO_2 in the feed stream at the inlet.

$$x=\frac{x_i-\frac{m}{n_{N_2}M_h}(1-x_i)}{1-\frac{m}{n_{N_2}M_h}(1-x_i)}; BC: x(0)=x_i \tag{4}$$

The reactor temperature is determined by solving the steady-state

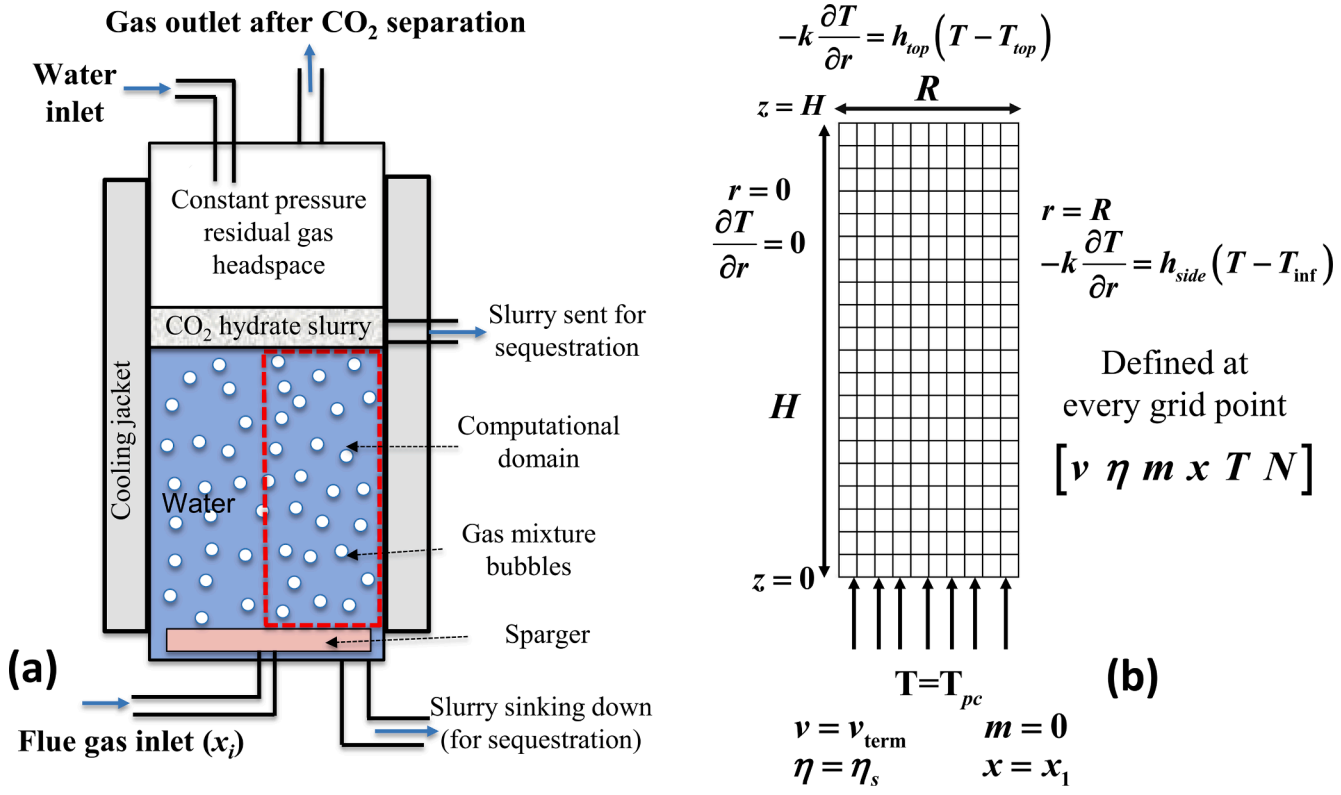

Fig. 1. (a) Schematic depiction of a continuously operating BCR for CO_2 hydrate formation, with the computational domain marked by the dotted boundary, (b) Boundary conditions associated with the computational domain. Figures adapted with permission from Ref. [52].

energy equation, which includes a term to account for heat generation from hydrate crystallization (Equation (5). In this study, the temperatures at the top (T_{top}) and side (T_{inf}) of the reactor and that of the incoming gas (T_{pc}) are all assumed to be the same as ambient, T_{amb}, and is the operating temperature of the system. Heat transfer coefficients are taken as 10 W/m^{2}K and 5000 W/m^{2}K at the top and sides of the reactor, respectively. The heat of formation for CO_2 hydrate (ΔH) is taken as 60 kJ/mol. Symmetry boundary condition is used at the centerline of the reactor ($r = 0$).

$$k\left(\frac{\partial^2 T}{\partial r^2} + \frac{1}{r}\frac{\partial T}{\partial r} + \frac{\partial^2 T}{\partial z^2}\right) + \frac{Nv\Delta H}{M_h}\frac{\partial m}{\partial z} = 0$$

$$BCs: T(0,r) = T_{amb}; -k\frac{\partial T}{\partial z}(H,r) = h_{top}(T(H,r) - T_{amb}) \quad (5)$$

$$-k\frac{\partial T}{\partial r}(z,0) = 0; -k\frac{\partial T}{\partial r}(z,R) = h_{side}(T(z,R) - T_{amb})$$

The number density of bubbles can be evaluated using a continuity equation without a source/sink term, since the model neglects bubble coalescence or bubble breakage (Equation (6). The pressure inside the reactor at any given height is evaluated using equation (7).

$$Nv = \frac{3Q}{4\pi\eta_s^3} \quad (6)$$

$$P(z) = P_{op} + \rho_w g(H - z) + \frac{2\gamma}{\eta(z)} \quad (7)$$

2.2. Output parameters

In order to evaluate the performance of the BCR, two key parameters are defined: i) gas consumption rate per unit reactor volume ($\dot{m}_{gcr}$), as defined in equation (8), and ii) percent conversion factor (η_{CF}) of participating incoming gas, as defined in equation (9). η_{CF} is defined as the ratio of moles of CO_2 consumed for hydrate formation inside the reactor to the moles of CO_2 in the incoming gas stream. The gas consumption rate directly determines the rate at which CO_2 is converted to hydrates, which can then be sent for CO_2 sequestration or CO_2 separation. This is a measure of the overall volumetric productivity or overall productivity of the system. On the other hand, the conversion factor is a measure of the system's efficiency in capturing CO_2 in a single pass. A low conversion factor means that the gas outlet stream will have higher CO_2 concentrations, necessitating recirculation. This would imply more BCRs functioning simultaneously, accompanied by compressors, intercoolers, etc., thereby increasing the overall cost. Upon assuming a fixed water replenishment rate with respect to gas flow rate into the system, a low efficiency would also imply higher water consumption for the same amount of CO_2 separated/sequestered as hydrate slurry, further increasing the cost. Overall, the operating conditions and the conversion factor largely determine the cost of the process, while the gas consumption rate determines its total value.

As the mass of hydrate on the bubble increases with axial distance, the total gas consumed also increases. The rate of gas consumption per unit reactor volume can therefore be estimated by evaluating the total consumption at the top of the domain ($z = H$) using equation (8). The result is reported in ton/yr/m^3, noting that such systems will run continuously. The total volume of the reactor is assumed as 110 % of the volume of the water in the BCR; the extra 10 % is the volume of headspace. The influence of operational and design parameters like P_{op}, T_{amb}, x_i, Q, H, and D on both performance metrics is quantified in this study. Simulations are conducted in the P-T region where CO_2 remains in the gas phase, water remains in liquid phase and the CO_2-water-hydrate thermodynamic stability is ensured.

$$\dot{m}_{gcr} = \int_0^R \frac{M_{CO_2}}{V_R M_h} N(H,r)v(H,r)m(H,r)2\pi r dr \quad (8)$$

$$\eta_{CF}(\%) = 100\frac{\dot{m}_{gcr}}{M_{CO_2} Q A_{cs} x_i P(0)/RT(0)} \quad (9)$$

3. Results and discussions

3.1. Influence of pressure and temperature on CO_2 hydrate formation

A CO_2/N_2 mixture (50/50 mol ratio), and an inlet gas flow rate of 67.5 ml/s was considered for a cylindrical reactor (height:10 m, diameter: 2 m); this is typical of reactor sizes for industrial applications [17]. It is seen that increasing the pressure and reducing the temperature increases both gas consumption rate and conversion factor (Fig. 2). This is due to an increase in subcooling from hydrate equilibrium which leads to a higher driving force, as per equation (3). While a temperature reduction continues to significantly increase the conversion factor, the increase in conversion factor due to increasing pressure stagnates at a temperature-dependent pressure. On the other hand, the gas consumption rate shows a linear increase with increasing pressure. This implies that a BCR's efficiency in separating CO_2 will stagnate beyond a certain pressure; however, the rate at which CO_2 hydrates can be formed will still continue to rise with increasing pressure. The best working condition in Fig. 2 shows a conversion factor of 34 % for $T_{amb} = 1$ °C and $P_{op} =$ 7 MPa. This means that 34 % of the inlet CO_2 can be converted to hydrate slurry and sent for sequestration while the rest would need separation via recirculation or via a different process. This corresponds to a gas consumption rate of $\sim$ 1.5 ton/yr/m^3 and implies that this BCR design will circumvent the cost of separating 1.5 ton/yr/m^3 of CO_2 from an otherwise impure stream before eventual sequestration (since CO_2 hydrates can be directly sequestered without further purification needed).

While Fig. 2 quantifies the benefits of higher pressure and lower temperatures, it should be noted that increasing pressure and reducing temperatures will also increase overall costs. Higher pressure requirements increase the compression (for gas) and pumping (for water). It also means that a higher mass flow rate would be needed to obtain the same volumetric gas flow rate at a higher pressure, further increasing the compression costs. Lowering temperatures increases the refrigeration requirements. It is noted that an additional gas consumption rate of $\sim$ 0.5 ton/yr/m^3 is obtained upon reducing the operating temperature by 2 °C. The rise in gas consumption rate is $\sim$ 30 % of the maximum value reported in Fig. 2. The marginal increase in refrigeration cost for an additional 2 °C cooling is not expected to be very significant, highlighting the advantages of low-temperature operation. Using saltwater will allow the system to operate at even lower temperatures. The higher conversion factor associated with high pressure and low temperature suggests that the hydrate slurry will contain more mass of CO_2 per mass of water, reducing water requirements and associated costs. The need for CO_2 recirculation and the cost of the corresponding infrastructure will also reduce when the system is operating at a higher pressure.

3.2. Influence of inlet mole fraction on CO_2 hydrate formation

To study the influence of inlet mole fraction, an ambient temperature of 1 °C and an inlet gas flow rate of 67.5 ml/s was considered for the previously described reactor. The operating pressure was varied from 4 to 10 MPa, and the corresponding CO_2 mole fraction at inlet was varied from 0.15 to 0.55 (Fig. 3). This range was selected to keep CO_2 in gaseous phase and also stay within hydrate forming conditions. A linear increase in gas consumption rate with increasing inlet mole fraction is seen; the slope slightly increased with increased pressure. For 10 MPa, increasing inlet concentration from 15 % to 35 % increases the total gas consumption rate tenfold. At the same time, a higher concentration feed stream will not change the cost associated with refrigeration, compression, etc.; the cost increase would be for increasing the concentration in feed streams (whether it be hydrates-based or another purification process). The obtained hydrate slurry from higher concentration inlet gas will also contain more CO_2 per unit mass of water.

On the other hand, although the conversion factor increases with increasing inlet mole fraction, a stagnation in conversion factor is seen (Fig. 3). This indicates that the system's efficiency in separating CO_2 stagnates above certain inlet mole fractions (e.g. 35–40 % for 10 MPa). This suggests that further purifying the stream after > 35–40 % gives significantly reduced benefits as the recirculation costs stay the same. This highlights the importance of hydrates-based CCS for medium purity CO_2 streams.

3.3. Influence of inlet gas flow rate (at various inlet mole fractions) on CO_2 hydrate formation

The influence of inlet gas flow rate at various inlet mole fractions was studied for the previously described reactor at a pressure of 10 MPa and temperature of 1 °C. For low inlet mole fractions (e.g., 0.15), the two performance parameters do not change substantially with the flow rate. For a fixed flow rate, both the parameters increase with increasing mole fraction, as also seen in Fig. 3. Fig. 4 shows that the gas consumption rate increases while the conversion factor reduces with increasing gas flow rate. The lowest flow rate corresponds to the highest conversion factor of 67.8 %, at an inlet mole fraction of 45 %. This is expected since higher

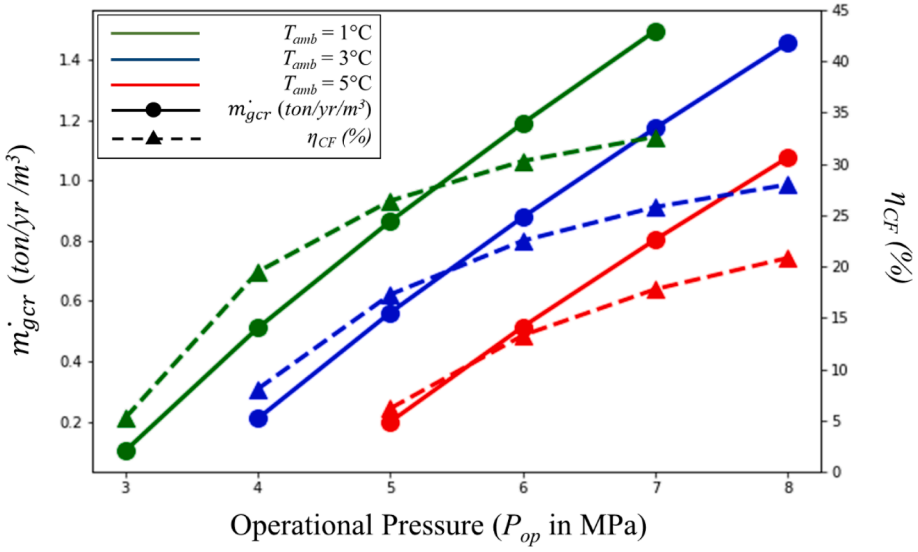

Fig. 2. Influence of operating pressure and temperature on key performance parameters for $x_i = 0.5$, $\dot{Q} = 67.5$ ml/s, $H = 10$ m and $D = 2$ m.

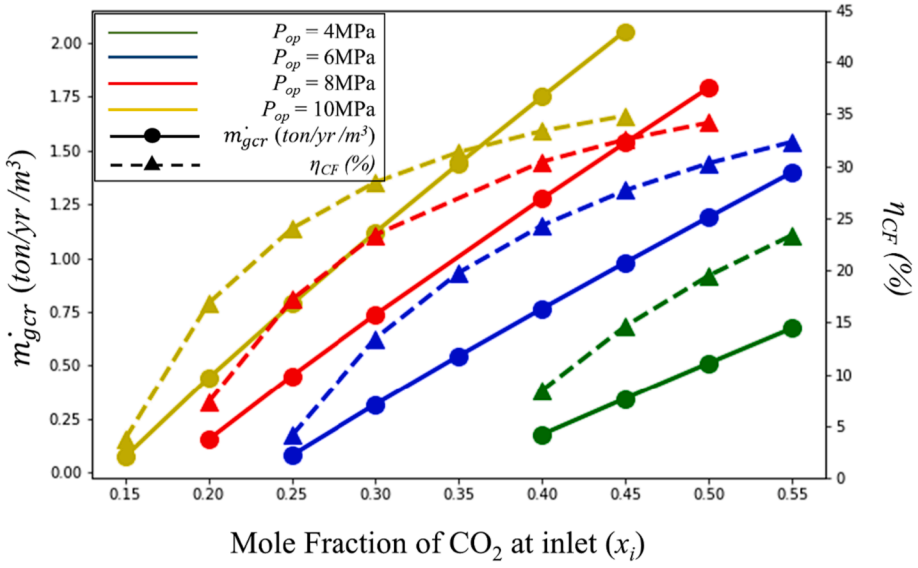

Fig. 3. Influence of operating pressure and inlet mole fraction on key performance parameters for T_{amb} = 1 °C, $\dot{Q}$ = 67.5 ml/s, H = 10 m and D = 2 m.

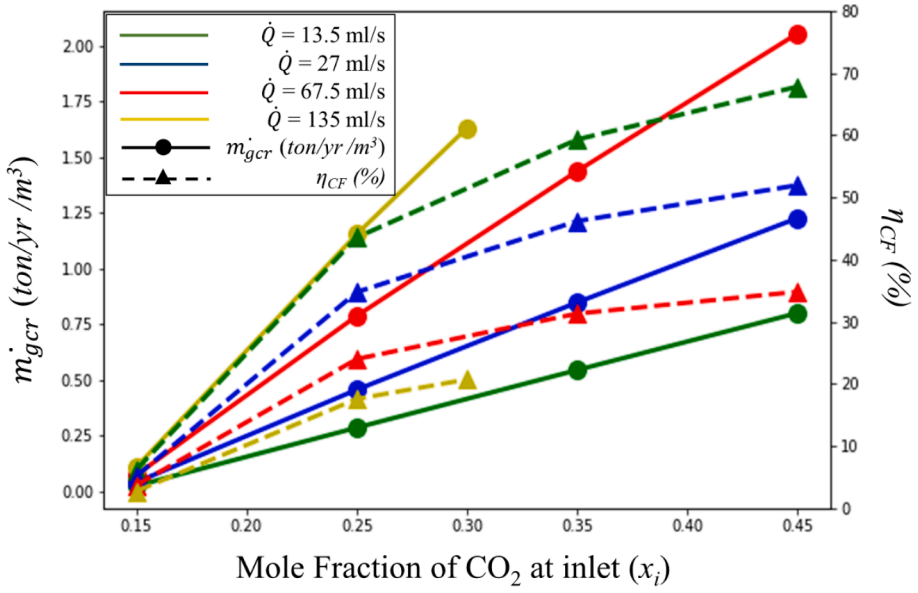

Fig. 4. Influence of inlet gas flow rate and inlet mole fraction on key performance parameters for T_{amb} = 1 °C, P_{op} = 10 MPa, H = 10 m and D = 2 m.

gas flow rates enhance turbulence-based heat dissipation and mass transfer in addition to increasing the amount of gas available for hydrate formation, leading to an increase in gas consumption rate. However, higher gas flow rates reduce the residence time of individual bubbles resulting in a lower conversion factor. This corresponds to a higher water requirement per amount of CO_2 converted into hydrate slurry. A higher flow rate is also accompanied by higher compression and refrigeration costs. The reduced conversion factor also implies an increase in the costs associated with recirculation. This means that the BCR should be run at low gas flow rates if the goal is to separate CO_2 from flue gas efficiently in a single-pass BCR. On the other hand, if the corresponding cost increases at a higher flow rate are minimal, it should be run at high flow rates to rapidly form hydrates thereby separating/sequestering the CO_2. In addition to the flow rate, the gas consumption rate also increases linearly with mole fraction. It is noted that operation of a BCR for CO_2 sequestration will typically involve high purity CO_2 feed streams. All these factors indicate that a BCR should be operated at high gas flow rates for CO_2 sequestration applications. However, this approach will increase recirculation-related costs and complexities due to a reduced conversion factor. A preliminary analysis on this aspect is presented in section 3.5. The optimum operating conditions can be decided based on a techno-economic analysis, which factors technical aspects alongside the economic implications of the technical solutions.

3.4. *Influence of reactor size on CO_2 hydrate formation*

The influence of reactor size was investigated for an operating pressure of 10 MPa, ambient temperature of 1 °C, inlet gas flow rate ($\dot{Q}$) of 67.5 ml/s, and inlet mole fraction of 0.15 and 0.35; results are presented in Figs. 5 and 6. It is seen that increasing the height or diameter increases the conversion factor. Increasing the height allows the bubbles to stay within the reactor for longer, which increases the conversion factor. A larger diameter reduces the area flux of the inlet gas; the gas is more spread out within the reactor, which facilitates heat dissipation leading to a higher conversion factor. This increase was much more prominent for higher inlet mole fractions. This effect is not equally

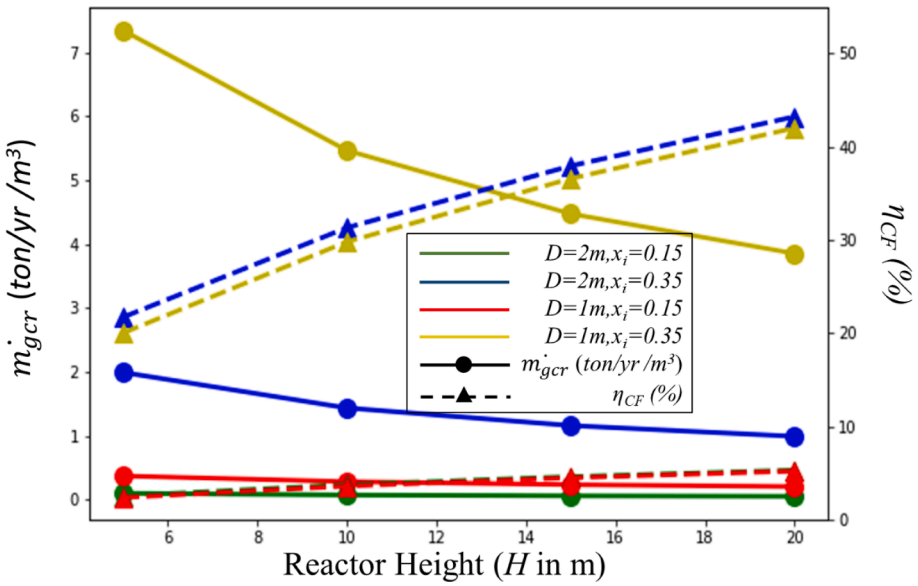

Fig. 5. Influence of reactor height (H) on key performance parameters for T_{amb} = 1 °C, P_{op} = 10 MPa and $\dot{Q}$ = 67.5 ml/s.

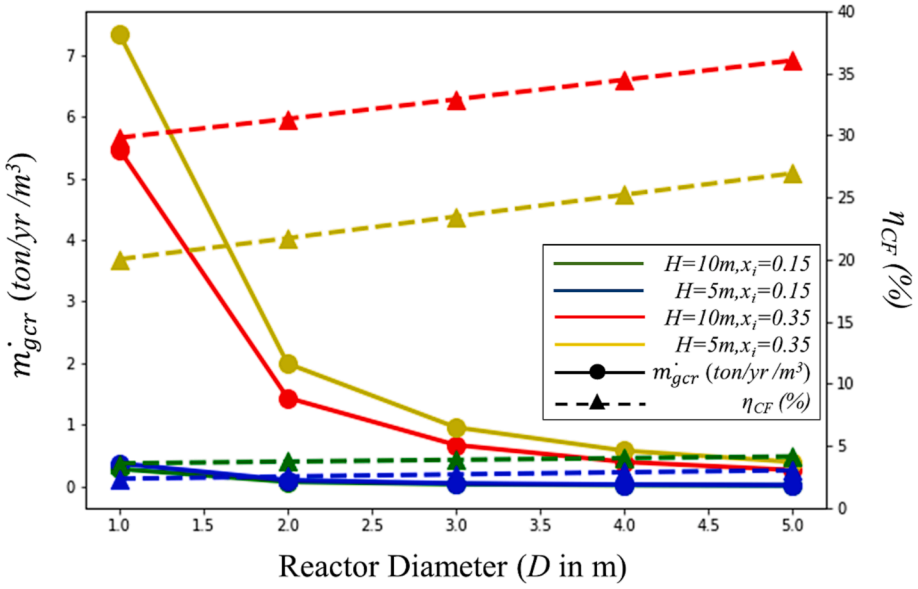

Fig. 6. Influence of reactor diameter (D) on key performance parameters for T_{amb} = 1 °C, P_{op} = 10 MPa and $\dot{Q}$ = 67.5 ml/s.

prominent for lower mole fractions because for $x_i = 0.15$, hydrate formation is limited by the lack of CO_2 in the gas mixture, and not by small residence time or ineffective heat dissipation. It is also noted that although the conversion factor increases with reactor volume (resulting from an increase in both height and diameter), the increase is only 20–30 % for a height increase of 50–100 %. This implies that while increasing the reactor volume will improve gas separation, it may not be economically beneficial owing to higher costs associated with larger reactors.

An increase in conversion factor (from the use of a taller reactor) will reduce the need for recirculation, thereby reducing costs associated with compression and refrigeration. Furthermore, for a given gas flow rate, the water requirement will be lower, reducing water costs as well. This also means that the hydrate slurry generated from a larger reactor will have a higher CO_2 mass fraction, increasing its pumping costs etc. accordingly. On the other hand, the volumetric gas consumption rate reduces with increasing height or diameter. This is because even though the overall hydrate formation increases upon increasing reactor volume, it does not increase linearly with volume. This is due to the fact that as CO_2 is removed from the gas mixture, the driving force for hydrate formation (due to difference in CO_2 concentrations presented in equation (3) reduces, thereby decreasing the rate of hydrate formation with height. The rapid increase in volumetric gas consumption rate upon decreasing the reactor volume suggests that compact BCRs will perform better if recirculation-associated costs are lower than the cost increase due to a larger reactor. The effect was more prominent for higher mole fractions due to the increase in available CO_2 for hydrate formation. This suggests that sequestration applications that aim to maximize volumetric production of hydrates will perform better for smaller reactors, as discussed in section 3.5.

3.5. Influence of reactor size and flow rate on CO_2 hydrate formation with pure CO_2

This sub-section analyzes hydrate formation with pure CO_2, an inlet mole fraction of 0.99 was used in the simulations. Temperature and pressure of 1 °C and 3 MPa was considered for two flow rates, 27 and 135 ml/s, and a bubble size of 250 μm. Figs. 7 and 8 show the influence of reactor height and reactor diameter on hydrate formation for a height range of 2.5–10 m, and a diameter range of 0.25–2 m. This range was selected based on the discussion in Section 3.4 which suggests that sequestration applications will perform better (on a volumetric basis) for a lower reactor volume. A taller reactor increases the residence time of gas. However, since pure CO_2 is being considered, the driving force for hydrate formation does not reduce with height as was observed for CO_2/N_2 mixtures. This results in a nearly constant volumetric gas consumption rate along the reactor height as shown in Fig. 7. The volumetric gas consumption was also observed to increase with increasing flow rate and reduced diameter. An increase of 5x in flow rate resulted in a nearly 3 times increase in gas consumption rate. However, it should be noted that although the total hydrate formation increases with increasing height or flow rate, it will also increase the total cost.

On the other hand, the volumetric gas consumption rate increases with smaller diameters (Fig. 8). This is because a reduced diameter increases gas flux, thereby ensuring more availability of CO_2 for hydrate formation per unit area. Smaller diameters also increase turbulence and mixing. The increase in gas consumption rate with reduced diameters is more prominent for higher flow rates. A 2.5x increase in gas consumption rate was observed for a 5x increase in gas flow rate. This translates to 28.9 ton/yr/m^3 which is the highest gas consumption rate reported in this study. The increase in gas consumption rate with reduced diameters is the same for a 5 m reactor and a 10 m reactor. From a techno-economic perspective, a higher flow rate will also increase the costs of compression, refrigeration and recirculation. A holistic assessment of the benefits of increasing flow rate can be provided via a techno-economic analysis, which is facilitated by this study.

Increasing the reactor height linearly increases the conversion factor (Fig. 7). This means that if the costs associated with a taller reactor do not increase substantially, longer reactors are better, as the other performance parameter is constant which implies that the total production will increase linearly with height, while the need for recirculation decreases. A reduced flow rate also increases conversion factor as was also observed for flue gas mixtures. Reducing the flow rate decreases the operating costs by reducing compression and recirculation-related costs. The water consumption per amount of CO_2 converted to hydrate slurry decreases with increasing height and decreasing flow rate. This means that if the cost of water is a significant factor in the techno-economic analysis, then a taller reactor with lower flow rates will be most attractive from a water utilization standpoint. The influence of diameter on conversion factor is shown in Fig. 8; it is seen that the conversion factor is nearly constant for the range of diameters considered. This implies that spreading out the gas within the reactor volume does not help in increasing total hydrate formation significantly. This suggests that the system is mass transfer limiting and not heat transfer limiting. This also implies that the costs for recirculation, water requirements and refrigeration will not change significantly with diameter. Increasing the diameter will increase the amount of material used, thereby driving up the costs. However, this material can be better used to increase height as the benefits of increasing the height on conversion factor are much higher than increasing the diameter (Figs. 7 and 8).

Overall, the trends associated with varying reactor height and diameter suggest that a high aspect ratio reactor is more favorable for hydrate formation, especially for sequestration applications, where the trends were more prominent when pure CO_2 was considered. This finding is expected since this model does not account for bubble–bubble interaction. In actual BCRs, bubble–bubble interactions like hydrate shell coalescence and subsequent bubble dissociation would be much higher for high aspect ratio reactors, which can result in issues like plugging, reduced gas-water surface area, etc.

4. Conclusions

The performance of a bubble column reactor for CO_2 hydrate formation from flue gas (mixture of CO_2/N_2) and pure CO_2 is modeled and quantified using two performance metrics: gas consumption (hydrate formation) rate per unit reactor volume and conversion factor (of inlet CO_2). The first metric quantifies the overall volumetric output of the reactor for CCS applications, while the second metric along with the operating conditions determines the cost to run the reactor. Conversion factor also determines the amount of water required and the concentration of the hydrate slurry that will be obtained. It is seen that increasing the reactor pressure and reducing temperature improves both the metrics. Hydrate formation rate also increases with increasing inlet mole fraction of CO_2. Increasing the gas flow rate increases the gas consumption rate but reduces the conversion factor. For flue gas

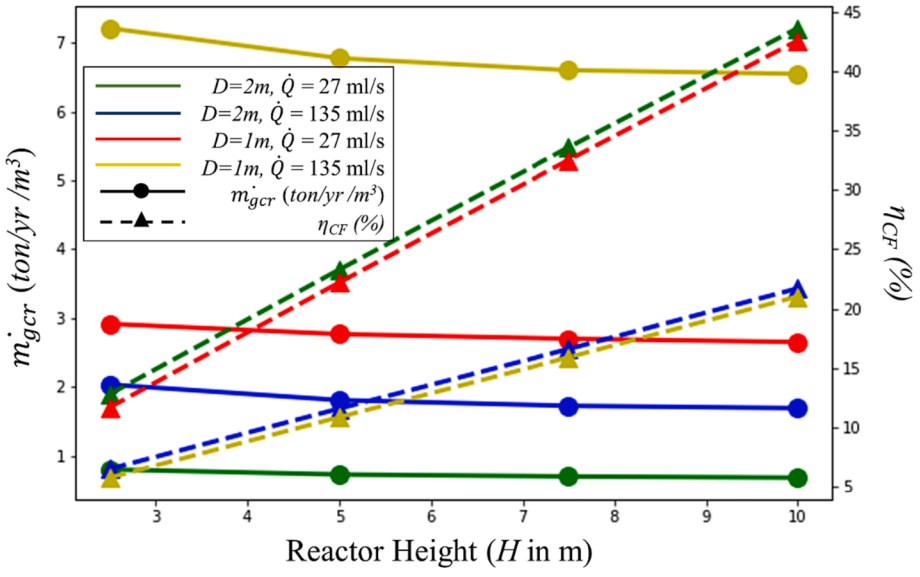

Fig. 7. Influence of reactor height (H) on key performance parameters for T_{amb} = 1 °C, P_{op} = 3 MPa and x_i = 0.99.

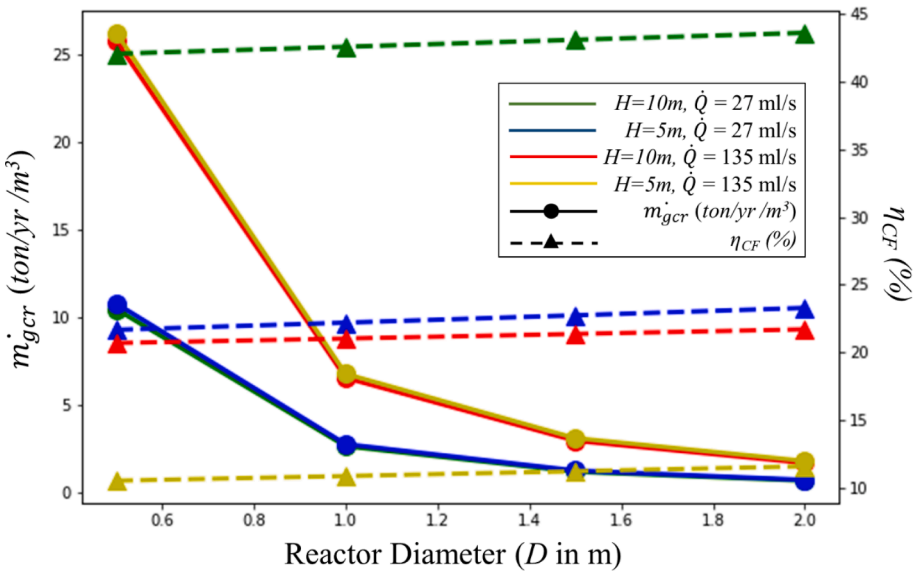

Fig. 8. Influence of reactor diameter (D) on key performance parameters for T_{amb} = 1 °C, P_{op} = 3 MPa and x_i = 0.99.

mixtures, increasing the channel height and diameter increases the conversion factor but reduces hydrate formation rate per unit reactor volume. For pure CO_2, conversion factor linearly increases with height and stays constant with increasing diameter. The volumetric gas consumption rate was height-independent but increased significantly with increasing diameter, resulting in a maximum gas consumption rate of 28.9 ton/yr/m^3. This suggests that taller BCRs with smaller diameters (high aspect ratio) are more suitable for CO_2 sequestration applications, whereas larger BCRs are more suitable for CO_2 separation applications. Overall, this study examines various quantitative and qualitative aspects of BCR operations and sets the stage for optimization and techno-economic analysis of CO_2 hydrates-based CCS approaches which use BCRs.

CRediT authorship contribution statement

Awan Bhati: Conceptualization, Methodology, Data curation, Writing – original draft. **Aritra Kar:** Conceptualization. **Vaibhav Bahadur:** Supervision, Writing – review & editing.

Declaration of Competing Interest

The authors declare the following financial interests/personal relationships which may be considered as potential competing interests: Vaibhav Bahadur reports financial support was provided by National Science Foundation.

Vaibhav Bahadur has patent #Methods and systems for promoting formation of CO2 clathrate hydrates by the use of magnesium and other active metals pending to The University of Texas at Austin.

Vaibhav Bahadur has patent #Systems and methods for formation, compaction, sealing and disposal of CO2 hydrates on the seabed pending to The University of Texas at Austin.

Awan Bhati has patent #Methods and systems for promoting formation of CO2 clathrate hydrates by the use of magnesium and other active metals pending to The University of Texas at Austin.

Awan Bhati has patent #Systems and methods for formation, compaction, sealing and disposal of CO2 hydrates on the seabed pending to The University of Texas at Austin.

Aritra Kar has patent #Methods and systems for promoting formation of CO2 clathrate hydrates by the use of magnesium and other active metals pending to The University of Texas at Austin.

Data availability

Data will be made available on request.

Acknowledgements

This study was supported by NSF grants 2234604, 1653412 and 2202071. Discussions with Prof. George Biros at UT Austin on various aspects of numerical solutions of the system of equations are acknowledged. The authors also acknowledge UT Austin Energy Institute and Texas Advanced Computing Center (TACC) at the University of Texas at Austin for providing high performance computing resources that contributed to the simulation results reported in this paper.

References

[1] H.J. Schellnhuber, S. Rahmstorf, R. Winkelmann, Why the right climate target was agreed in Paris, Nat. Clim. Chang. 6 (7) (2016) 649–653, https://doi.org/10.1038/nclimate3013.
[2] United Nations, *Emissions Gap Report 2022: The Closing Window*. 2022.
[3] IPCC, *Carbon dioxide capture and storage*, vol. 58. 2005.
[4] V. Belandria, A.H. Mohammadi, A. Eslamimanesh, D. Richon, M.F. Sánchez-Mora, L.A. Galicia-Luna, Phase equilibrium measurements for semi-clathrate hydrates of the (CO 2+N 2+tetra-n-butylammonium bromide) aqueous solution systems: Part 2, Fluid Phase Equilib. 322–323 (2012) 105–112, https://doi.org/10.1016/j.fluid.2012.02.020.
[5] A.M. Gambelli, A. Presciutti, F. Rossi, Review on the characteristics and advantages related to the use of flue-gas as CO2/N2 mixture for gas hydrate production, Fluid Phase Equilib. 541 (2021), 113077, https://doi.org/10.1016/j.fluid.2021.113077.
[6] R.T.J. Porter, M. Fairweather, M. Pourkashanian, R.M. Woolley, The range and level of impurities in CO2 streams from different carbon capture sources, Int. J. Greenh. Gas Control 36 (2015) 161–174, https://doi.org/10.1016/j.ijggc.2015.02.016.
[7] S. Roussanaly, C. Fu, M. Voldsund, R. Anantharaman, M. Spinelli, M. Romano, Techno-economic Analysis of MEA CO2 Capture from a Cement Kiln - Impact of Steam Supply Scenario, Energy Proc. 114 (1876) (2017) 6229–6239, https://doi.org/10.1016/j.egypro.2017.03.1761.
[8] D. Berstad, R. Anantharaman, P. Nekså, Low-temperature CO2 capture technologies - Applications and potential, Int. J. Refrig. 36 (5) (2013) 1403–1416, https://doi.org/10.1016/j.ijrefrig.2013.03.017.
[9] E. D. S. Jr, "Fundamental principles and applications of natural gas hydrates," vol. 426, no. November, pp. 353–359, 2003.
[10] E. D. Sloan and C. A. Koh, *Clathrate Hydrates of Natural Gases*. 2008.
[11] J. J. Carroll, *Natural Gas Hydrates: A Guide for Engineers, Second Edition*, no. October. 2009.
[12] A. Hassanpouryouzband, et al., Gas hydrates in sustainable chemistry, Chem. Soc. Rev. 49 (15) (2020) 5225–5309, https://doi.org/10.1039/c8cs00989a.
[13] L.C. Ho, P. Babu, R. Kumar, P. Linga, HBGS (hydrate based gas separation) process for carbon dioxide capture employing an unstirred reactor with cyclopentane, Energy 63 (2013) 252–259, https://doi.org/10.1016/j.energy.2013.10.031.

[14] J. Zheng, Z.R. Chong, M.F. Qureshi, P. Linga, Carbon Dioxide Sequestration via Gas Hydrates: A Potential Pathway toward Decarbonization, Energy and Fuels 34 (9) (2020) 10529–10546, https://doi.org/10.1021/acs.energyfuels.0c02309.
[15] A. Adeyemo, R. Kumar, P. Linga, J. Ripmeester, P. Englezos, Capture of carbon dioxide from flue or fuel gas mixtures by clathrate crystallization in a silica gel column, Int. J. Greenh. Gas Control 4 (3) (2010) 478–485, https://doi.org/10.1016/j.ijggc.2009.11.011.
[16] P. Wang, Y. Teng, Y. Zhao, J. Zhu, Experimental Studies on Gas Hydrate-Based CO2 Storage: State-of-the-Art and Future Research Directions, Energy Technol. 9 (7) (2021) 1–11, https://doi.org/10.1002/ente.202100004.
[17] A. Bhati, M. Lokanathan, S. Smaha, and V. Bahadur, "Interviews of Industry Professionals as part of NSF I-Corps Program." 2022.
[18] X. Cao, Y. Su, Y. Liu, J. Zhao, C. Liu, Storage capacity and vibration frequencies of guest molecules in CH 4 and CO2 hydrates by first-principles calculations, J. Phys. Chem. A 118 (1) (2014) 215–222, https://doi.org/10.1021/jp408763z.
[19] IEA GHG, "Gas Hydrates for Deep Ocean Storage of Co2 - Hydrates for Transportation and Deep Ocean Storage of Co2 - Background to the Study," *IEA Greenh. Gas R&D Program. Rep. PH4/26*, no. February, 2004.
[20] L. Bernardes, J. Carneiro, P. Madureira, F. Brandão, C. Roque, Determination of priority study areas for coupling CO2 storage and CH4 gas hydrates recovery in the Portuguese offshore area, Energies 8 (9) (2015) 10276–10292, https://doi.org/10.3390/en80910276.
[21] N. Goel, In situ methane hydrate dissociation with carbon dioxide sequestration: Current knowledge and issues, J. Pet. Sci. Eng. 51 (3–4) (2006) 169–184, https://doi.org/10.1016/j.petrol.2006.01.005.
[22] L. Zhang, et al., Enhanced CH4 recovery and CO2 storage via thermal stimulation in the CH4/CO2 replacement of methane hydrate, Chem. Eng. J. 308 (2017) 40–49, https://doi.org/10.1016/j.cej.2016.09.047.
[23] K.P.L.T. Austvik, DEPOSITION OF CO2 ON THE SEABED IN THE FORM OF HYDRATES, Energy Convers. Mgm 33 (5) (1992) 659–666.
[24] H. Lee, Y. Seo, Y.-T. Seo, I.L. Moudrakovski, J.A. Ripmeester, Recovering Methane from Solid Methane Hydrate with Carbon Dioxide, Angew. Chemie 115 (41) (2003) 5202–5205, https://doi.org/10.1002/ange.200351489.
[25] R.P. Warzinski, R.J. Lynn, G.D. Holder, The impact of CO2 clathrate hydrate on deep ocean sequestration of CO2. Experimental observations and modeling results, Ann. N. Y. Acad. Sci. 912 (2000) 226–234, https://doi.org/10.1111/j.1749-6632.2000.tb06776.x.
[26] D. Riestenberg, E. Chiu, M. Gborigi, L. Liang, O.R. West, C. Tsouris, Investigation of jet breakup and droplet size distribution of liquid CO2 and water systems-implications for CO2 hydrate formation for ocean carbon sequestration, Am. Minerol. 89 (2004) 1240–1246.
[27] P. Babu, P. Linga, R. Kumar, P. Englezos, A review of the hydrate based gas separation (HBGS) process forcarbon dioxide pre-combustion capture, Energy 85 (2015) 261–279, https://doi.org/10.1016/j.energy.2015.03.103.
[28] P. Wang, et al., Review on the synergistic effect between metal–organic frameworks and gas hydrates for CH4 storage and CO2 separation applications, Renew. Sustain. Energy Rev. vol. 167, no. August (2022), 112807, https://doi.org/10.1016/j.rser.2022.112807.
[29] C.G. Xu, X. Sen Li, Q.N. Lv, Z.Y. Chen, J. Cai, Hydrate-based CO2 (carbon dioxide) capture from IGCC (integrated gasification combined cycle) synthesis gas using bubble method with a set of visual equipment, Energy 44 (1) (2012) 358–366, https://doi.org/10.1016/j.energy.2012.06.021.
[30] Z. Chen, J. Fang, C. Xu, Z. Xia, K. Yan, Carbon dioxide hydrate separation from Integrated Gasification Combined Cycle (IGCC) syngas by a novel hydrate heat-mass coupling method, Energy 199 (2020), 117420, https://doi.org/10.1016/j.energy.2020.117420.
[31] G. Yue *et al.*, "Combining Di ff erent Additives with TBAB on CO 2 Capture and CH 4 Puri fi cation from Simulated Biogas Using Hydration Method," 2019, doi: 10.1021/acs.jced.8b01188.
[32] J. Lim, W. Choi, J. Mok, Y. Seo, Kinetic CO 2 selectivity in clathrate-based CO 2 capture for upgrading CO 2 - rich natural gas and biogas, Chem. Eng. J. 369 (January) (2019) 686–693, https://doi.org/10.1016/j.cej.2019.03.117.
[33] J. Yi, D. Zhong, J. Yan, and Y. Lu, "Impacts of the surfactant sulfonated lignin on hydrate based CO 2 capture from a CO 2 / CH 4 gas mixture," vol. 171, pp. 61–68, 2019, doi: 10.1016/j.energy.2019.01.007.
[34] X. Zang, L. Wan, Y. He, D. Liang, CO 2 removal from synthesized ternary gas mixtures used hydrate formation with sodium dodecyl sulfate (SDS) as additive, Energy 190 (2020), 116399, https://doi.org/10.1016/j.energy.2019.116399.
[35] S. Fan, S. Li, J. Wang, X. Lang, Y. Wang, Efficient capture of CO2 from simulated flue gas by formation of TBAB or TBAF semiclathrate hydrates, Energy and Fuels 23 (8) (2009) 4202–4208, https://doi.org/10.1021/ef9003329.
[36] J. Zheng, K. Bhatnagar, M. Khurana, P. Zhang, B. Y. Zhang, and P. Linga, "Semiclathrate based CO2 capture from fuel gas mixture at ambient temperature: Effect of concentrations of tetra-n-butylammonium fluoride (TBAF) and kinetic additives," *Appl. Energy*, vol. 217, no. October 2017, pp. 377–389, 2018, doi: 10.1016/j.apenergy.2018.02.133.
[37] P. Linga, R. Kumar, P. Englezos, Gas hydrate formation from hydrogen/carbon dioxide and nitrogen/carbon dioxide gas mixtures, Chem. Eng. Sci. 62 (16) (2007) 4268–4276, https://doi.org/10.1016/j.ces.2007.04.033.
[38] J. Xu, J. Cheng, K. Xin, J. Xu, W. Yang, Developing a Spiral-Ascending CO 2 Dissolver to Enhance CO 2 Mass Transfer in a Horizontal Tubular Photobioreactor for Improved Microalgal Growth, ACS Sustain. Chem. Eng. 8 (2020) 18926–18935, https://doi.org/10.1021/acssuschemeng.0c06124.
[39] Z.W. Ma, P. Zhang, H.S. Bao, S. Deng, Review of fundamental properties of CO2 hydrates and CO2 capture and separation using hydration method, Renew. Sustain. Energy Rev. 53 (2016) 1273–1302, https://doi.org/10.1016/j.rser.2015.09.076.
[40] A. Li, J. Wang, B. Bao, High-efficiency CO2 capture and separation based on hydrate technology: A review, Greenh. Gases Sci. Technol. 9 (2) (2019) 175–193, https://doi.org/10.1002/ghg.1861.
[41] S.P. Kang, H. Lee, B.J. Ryu, Enthalpies of dissociation of clathrate hydrates of carbon dioxide, nitrogen, (carbon dioxide + nitrogen), and (carbon dioxide + nitrogen + tetrahydrofuran), J. Chem. Thermodyn. 33 (5) (2001) 513–521, https://doi.org/10.1006/jcht.2000.0765.
[42] F. Zhang, S.K. Bhatia, B. Wang, B. Chalermsinsuwan, X. Wang, Experimental and numerical study on the kinetics of CO2–N2 clathrate hydrates formation in silica gel column with dodecyltrimethylammonium chloride for effective carbon capture, J. Mol. Liq. 363 (2022), 119764, https://doi.org/10.1016/j.molliq.2022.119764.
[43] S. Wang, et al., Methionine aqueous solution loaded vermiculite/MXene aerogels for efficient CO2 storage via gas hydrate, Fuel 334 (P2) (2023), 126833, https://doi.org/10.1016/j.fuel.2022.126833.
[44] H. Liu, et al., Clay nanoflakes and organic molecules synergistically promoting CO2 hydrate formation, J. Colloid Interface Sci. 641 (2023) 812–819, https://doi.org/10.1016/j.jcis.2023.03.118.
[45] P. Linga, N. Daraboina, J.A. Ripmeester, P. Englezos, Enhanced rate of gas hydrate formation in a fixed bed column filled with sand compared to a stirred vessel, Chem. Eng. Sci. 68 (1) (2012) 617–623, https://doi.org/10.1016/j.ces.2011.10.030.
[46] G. Li, D. Liu, Y. Xie, Y. Xiao, Study on effect factors for CO2 hydrate rapid formation in a water-spraying apparatus, Energy and Fuels 24 (8) (2010) 4590–4597, https://doi.org/10.1021/ef100417y.
[47] X. Zang, L. Wan, D. Liang, Investigation of the hydrate formation process in fine sediments by a binary CO2/N2 gas mixture, Chinese J. Chem. Eng. 27 (9) (2019) 2157–2163, https://doi.org/10.1016/j.cjche.2019.02.032.
[48] P. Linga, R. Kumar, J. Dong, J. Ripmeester, P. Englezos, A new apparatus to enhance the rate of gas hydrate formation : Application to capture of carbon dioxide, Int. J. Greenh. Gas Control 4 (2010) 630–637, https://doi.org/10.1016/j.ijggc.2009.12.014.
[49] S.S. Fan, G.J. Chen, Q.L. Ma, T.M. Guo, Experimental and modeling studies on the hydrate formation of CO2 and CO2-rich gas mixtures, Chem. Eng. J. 78 (2–3) (2000) 173–178, https://doi.org/10.1016/S1385-8947(00)00157-1.
[50] A. ur Rehman and B. Lal, "Gas Hydrate-Based CO2 Capture: A Journey from Batch to Continuous," *Energies*, vol. 15, no. 21, pp. 1–27, 2022, doi: 10.3390/en15218309.
[51] A. Elhambakhsh, M.R. Zaeri, M. Mehdipour, P. Keshavarz, Synthesis of different modified magnetic nanoparticles for selective physical / chemical absorption of CO 2 in a bubble column reactor, J. Environ. Chem. Eng. 8 (5) (2020), 104195, https://doi.org/10.1016/j.jece.2020.104195.
[52] A. Kar, V. Bahadur, Analysis of coupled heat & mass transfer during gas hydrate formation in bubble column reactors, Chem. Eng. J. 452 (P2) (2023), 139322, https://doi.org/10.1016/j.cej.2022.139322.
[53] Y.T. Luo, J.H. Zhu, S.S. Fan, G.J. Chen, Study on the kinetics of hydrate formation in a bubble column, Chem. Eng. Sci. 62 (4) (2007) 1000–1009, https://doi.org/10.1016/j.ces.2006.11.004.
[54] A. Kumar, A.V. Palodkar, R. Gautam, N. Choudhary, H.P. Veluswamy, S. Kumar, Role of salinity in clathrate hydrate based processes, J. Nat. Gas Sci. Eng. vol. 108, no. May (2022), 104811, https://doi.org/10.1016/j.jngse.2022.104811.
[55] A. Kar, V. Bahadur, Analysis of coupled heat & mass transfer during gas hydrate formation in bubble column reactors, Chem. Eng. J. 452 (2023) 1–26, https://doi.org/10.1016/j.cej.2022.139322.
[56] G.A. Melhem, R. Saini, B.M. Goodwin, A modified Peng-Robinson equation of state, Chem. Eng. Commun. 47 (1989) 189–237, https://doi.org/10.1080/00986449708936677.
[57] A. Kar, et al., Diffusion-based modeling of film growth of hydrates on gas-liquid interfaces, Chem. Eng. Sci. 234 (2021), 116456, https://doi.org/10.1016/j.ces.2021.116456.